

# Active network management for electrical distribution systems: problem formulation, benchmark, and approximate solution

Quentin Gemine<sup>\*</sup>, Damien Ernst<sup>\*</sup>, and Bertrand Cornélusse<sup>\*</sup>

<sup>\*</sup>{qgemine@ulg.ac.be, dernst@ulg.ac.be, bertrand.cornelusse@ulg.ac.be},  
Department of Electrical Engineering and Computer Science, University of Liège,  
4000 Liège, Belgium

July 17, 2015

## Abstract

With the increasing share of renewable and distributed generation in electrical distribution systems, Active Network Management (ANM) becomes a valuable option for a distribution system operator to operate his system in a secure and cost-effective way without relying solely on network reinforcement. ANM strategies are short-term policies that control the power injected by generators and/or taken off by loads in order to avoid congestion or voltage issues. While simple ANM strategies consist in curtailing temporary excess generation, more advanced strategies rather attempt to move the consumption of loads to anticipated periods of high renewable generation. However, such advanced strategies imply that the system operator has to solve large-scale optimal sequential decision-making problems under uncertainty. The problems are sequential for several reasons. For example, decisions taken at a given moment constrain the future decisions that can be taken, and decisions should be communicated to the actors of the system sufficiently in advance to grant them enough time for implementation. Uncertainty must be explicitly accounted for because neither demand nor generation can be accurately forecasted. We first formalize the ANM problem, which in addition to be sequential and uncertain, has a non-linear nature stemming from the power flow equations and a discrete nature arising from the activation of power modulation signals. This ANM problem is then cast as a stochastic mixed integer non-linear program, for which we provide quantitative results using state of the art open source solvers and perform a sensitivity analysis over the amount of flexibility available in the system and the number of scenarios considered in the deterministic equivalent of the stochastic program. To foster further research on this problem, we make available a test bed based on a 75-bus distribution network at <http://www.montefiore.ulg.ac.be/~anm/>. This test bed contains a simulator of the distribution system, with stochastic models for the generation and consumption devices, and callbacks to implement and test various ANM strategies.

**Index terms**— Active network management, electrical distribution network, flexibility services, renewable energy, optimal sequential decision-making under uncertainty, large system, Mixed Integer Non-linear Program.

## 1 Notation

We present here the main elements of notation used throughout the text. Some locally defined notation may not be covered in this section.

### Indices:

- $d$  Device connected to a node.
- $l$  Link of the electrical system.
- $m$  or  $n$  Node of the electrical system.
- $t$  Time period.

### Sets:

- $\mathcal{D}$  Set of electrical devices.
- $\mathcal{G}$  Subset of  $\mathcal{D}$  containing distributed generators.
- $\mathcal{C}$  Subset of  $\mathcal{D}$  that are electrical loads.
- $\mathcal{F}$  Subset of  $\mathcal{C}$  that can be controlled by the DSO.
- $\mathcal{T}$  Set of time periods.
- $\mathcal{N}$  Set of nodes of the electrical system.
- $\mathcal{L}$  Set of links of the electrical system.
- $\mathcal{S}_t^{(i)}$  Space of state vector  $\mathbf{s}_t^{(i)}$  (see the variables below for  $i \in \{1, 2, 3\}$ ).
- $\mathcal{S}$  Global state space of the system.
- $\mathcal{A}_s$  Feasible action (or control) space in state  $s \in \mathcal{S}$ .
- $\mathcal{A}_{d,s}^{(f)}$  Feasible set of  $a_{d,t}^{(f)}$  (see variables).
- $\mathcal{W}$  Set of possible realizations of random processes.

### Parameters:

- $Y_{mn}^{(br)}$  Branch admittance of link  $(m, n)$ .
- $Y_{mn}^{(sh)}$  Shunt admittance of link  $(m, n)$  on the side of node  $m$ .
- $t_{mn}$  Transformation ratio of link  $(m, n)$  on the side of node  $m$ .
- $\mathbf{Y}$  Nodal admittance matrix.
- $\mathbf{Y}_n$   $n^{\text{th}}$  row of  $\mathbf{Y}$ .
- $Y_{mn}$  Element  $(m, n)$  of  $\mathbf{Y}$ .
- $\underline{V}_n$  and  $\overline{V}_n$  Lower and upper operational limits on voltage magnitude  $|V_n|$ .
- $\overline{I}_l$  Operational limit on current magnitude  $|I_l|$ .
- $\tan \phi_d$  Reactive to active power ratio of device  $d$  (assumed constant for all devices).
- $T_d$  Duration of a modulation signal sent to a flexible load.

$\Delta P_d$	Vector of length $T_d$ representing the modulation signal sent to a flexible load.
$N_{loads}$	Length of the history of load consumption tracked in the state.
$N_{ir}$	Length of the history of solar irradiance tracked in the state.
$N_v$	Length of the history of wind speed tracked in the state.
$q_t$	Index of a quarter of an hour.

**Variables:** Note that some variables may have an additional subscript  $t$ . Also some variables are control variables, some represent the state of the system, and the remaining variables are exogenous stochastic processes.

$\mathbf{V}$	Vector of size $ \mathcal{N} $ , node voltages.
$V_n$	Complex voltage at node $n$ , i.e. $n^{\text{th}}$ component of $\mathbf{V}$ .
$\mathbf{I}$	Vector of size $ \mathcal{N} $ , current injected in the nodes.
$I_i$	If $i = l$ , it is the complex current in link $l$ , if $i = n$ , it is the complex current injected in bus $n$ , i.e. $n^{\text{th}}$ component of $\mathbf{I}$ .
$S_i$	Apparent power injected in bus. If $i = d$ , it is the power injected by device $d$ . If $i = n$ , it is the total power injected by all devices connected at node $n$ .
$P_i$	Active power injected in bus. If $i = d$ , it is the power injected by device $d$ . If $i = n$ , it is the total power injected by all devices connected at node $n$ .
$Q_i$	Reactive power injected in bus. If $i = d$ , it is the power injected by one device. If $i = n$ , it is the total power injected by all devices connected at node $n$ .
$S_{mn}$	Apparent power entering branch $l = (m, n)$ from the $m$ side.
$P_{mn}$	Active power entering branch $l = (m, n)$ from the $m$ side.
$Q_{mn}$	Reactive power entering branch $l = (m, n)$ from the $m$ side.
$ir_t$	Solar irradiance level at time $t$ .
$v_t$	Wind speed at time $t$ .
$\mathbf{s}_t^{(1)}$	Vector representing the state of the devices at time $t$ .
$\mathbf{s}_t^{(2)}$	Vector representing the state of the modulation instructions sent to controllable devices, at time $t$ .
$\mathbf{s}_t^{(f)}$	Vector representing the state of the flexible loads at time $t$ , it is a part of $\mathbf{s}_t^{(2)}$ .
$\mathbf{s}_t^{(3)}$	Part of the state of the system that, at time $t$ , keeps track of past realizations of the uncertain phenomena.
$\mathbf{s}_t$	Global state of the system at time $t$ .
$\mathbf{a}_t$	Vector of control actions taken at time $t$ .
$\bar{\mathbf{p}}_t$	Maximum level of active power injection for period $t+1$ and for each of the generators $g \in \mathcal{G}$ , part of $\mathbf{a}_t$ .

$\mathbf{a}_t^{(f)}$	Activation indicators of the flexibility services of the loads $d \in \mathcal{F}$ , part of $\mathbf{a}_t$ .
$a_{d,t}^{(f)}$	Component of $\mathbf{a}_t^{(f)}$ for flexible load $d \in \mathcal{F}$ .
$\mathbf{w}_t$	Information on exogenous phenomena available at time $t$ .

**Operators and functions:**

$ \cdot $	Magnitude of a complex number or size of a set.
$\cdot^*$	Complex conjugate.
$f : \mathcal{S} \times \mathcal{A}_s \times \mathcal{W} \rightarrow \mathcal{S}$	Transition function of the system.
$r : \mathcal{S} \times \mathcal{A}_s \times \mathcal{S} \rightarrow \mathbb{R}$	Reward function.
$\pi : \mathcal{S} \rightarrow \mathcal{A}_s$	Policy that returns an action for every feasible state.
$\mathcal{G}(n)$	Set of generators connected to node $n$ .
$\mathcal{C}(n)$	Set of loads connected to node $n$ .
$\mathcal{F}(n)$	Set of flexible loads connected to node $n$ .

## 2 Introduction

In Europe, the 20/20/20 objectives of the European Commission and the consequent financial incentives established by local governments are currently driving the growth of electricity generation from renewable energy sources [1]. A substantial part of the investments are made at the distribution networks (DN) level and consists of the installation of wind turbines or photovoltaic panels. The significant increase of the number of these distributed generators (DGs) undermines the *fit and forget* doctrine, which has dominated the planning and the operation of DNs up to now. This doctrine was developed when the energy was coming from the transmission network (TN) to the consumers, through the distribution network (DN). With this approach, adequate investments in network components (i.e., lines, cables, transformers, etc.) are made to avoid congestion and voltage issues, without requiring continuous monitoring and control of the power flows or voltages. To that end, network planning is done with respect to a set of critical scenarios gathering information about production and demand levels, in order to always ensure sufficient operational margins. Nevertheless, with the rapid growth of DGs, the preservation of such conservative margins implies significant network reinforcement costs, because the net energy flow may be reversed, from the distribution network to the transmission network, and flows within the distribution network be very different from the flows historically observed.

In order to avoid these potentially prohibitive costs, *active network management* (ANM) strategies have recently been proposed as alternatives to the fit and forget approach. The principle of ANM is to address congestion and voltage issues via short-term decision-making policies [2]. Frequently, ANM schemes maintain the system within operational limits in quasi real-time by relying on the curtailment of wind or solar generation [3, 4, 5]. Curtailment of renewable energy may, however, be very controversial from an environmental point of view and should probably be considered as a last resort. In that mindset, it is worth investigating ANM schemes that could also exploit the flexibility of

the loads, so as to decrease the reliance on generation curtailment. Exploiting flexible loads within an ANM scheme comes with several challenges. One such challenge is that modulating a flexible load at one instant is often going to influence its modulation range at subsequent instants. This is because flexible loads (e.g. heat pumps) are often constrained to consume a specific amount of energy over a certain duration. In this context, it is therefore important for a distribution system operator (DSO) not to take decisions by planning operations over a sufficiently long time horizon [6]. The uncertainty of future power injections from DGs relying on natural energy sources (wind, sun, *etc.*), as well as the uncertainty of the power consumption of the loads, should also be explicitly accounted for in the ANM strategy.

Many authors have already attempted to provide solutions to these operational planning problems. Since they rely on different formalisms, it is difficult for one author to rebuild on top of another's work. However, a thorough reading of these works suggests that it is possible to have a common decision paradigm, because these formalisms can be considered as an extension of the *optimal power flow* (OPF) problem [7]. More specifically, they can be assimilated to sequential decision-making problems where, at each time step, constraints that are similar to those used for defining an OPF problem are met. In this article, we aim to reduce the fragmentation of research efforts and facilitate the comparison of solution techniques that have been developed. To that end, we first propose a generic formulation of ANM related decision-making problems. More specifically, we detail a procedure to state these problems as Markov Decision Processes (MDP), where the system dynamics describes the evolution of the electrical network and devices, while the action space encompasses the control actions that are available to the DSO. Afterwards, we instantiate this procedure on a 75-bus network and use the elements of the resulting MDP to build a simulator of the system, which is available at <http://www.montefiore.ulg.ac.be/~anm/>. In this work we consider the operation of the medium-voltage (MV) network of the DSO, i.e. low voltage subnetworks are aggregated. We provide quantitative results for the resolution of the ANM problem casted as a stochastic mixed integer non-linear program (MINLP) using state of the art open source solvers. We then perform a sensitivity analysis over the amount of flexibility available in the system and the number of scenarios considered in the deterministic equivalent of the stochastic program.

The rest of this paper is structured as follows. The ANM problem of a DN is described in Section 3, where the electrical model and the network operation details are explained, and the operational planning problem is formulated as a Markov decision process. This formulation is then cast as a stochastic mixed-integer and non-linear program in Section 4. The benchmark built around a 75-bus test system is described in Section 5. Results obtained with an open source MINLP solver are presented in Section 6. Section 7 concludes and presents possible extensions of this work.

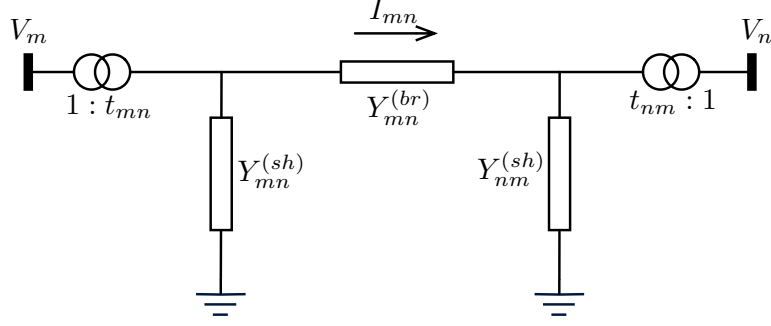


Figure 1:  $\pi$ -model of a link.

### 3 Problem Description

#### 3.1 Model of the electrical distribution system

In this paper, we are always considering that the network and all its devices are operating in alternating current mode. We also make the choice to represent complex numbers in rectangular coordinates.

The electrical distribution system can be mathematically represented by a graph, that is a set of nodes, and a set of links connecting nodes. A node is an electrical bus characterized by a voltage  $V_n \in \mathbb{C}$ . In addition to links connecting a bus to its neighbors, several devices may be connected to a bus. Devices are either injecting or withdrawing power. Every link  $(m, n) \in \mathcal{L} \subset \mathcal{N}^2$  connects a pair of nodes  $m, n \in \mathcal{N}$  and represents an overhead line, an underground cable, or a transformer. A link is represented by its  $\pi$ -model, composed of five complex parameters: two ratios  $t_{mn}$  and  $t_{nm}$ , a branch admittance  $Y_{mn}^{(br)}$ , and two shunt admittances  $Y_{mn}^{(sh)}$  and  $Y_{nm}^{(sh)}$  (see Fig. 1), that are considered fixed in this work, although opportunities to change them dynamically can exist in practice. More details on the  $\pi$ -model of specific links can be found in [8].

To ensure the proper operation of the devices connected to a bus, the voltage magnitude  $|V_n|$  at node  $n$  should not deviate too much from its nominal voltage level:

$$\forall n \in \mathcal{N} : \underline{V}_n \leq |V_n| \leq \overline{V}_n. \quad (1)$$

If  $I_{mn} \in \mathbb{C}$  is the branch current through link  $(m, n)$ , its magnitude  $|I_{mn}|$  should be kept below a pre-specified limit to prevent excessive heating of conductors and insulating materials:

$$\forall (m, n) \in \mathcal{L} : |I_{mn}| \leq \overline{I}_{mn}. \quad (2)$$

In reality, there are several limits depending on the magnitude and duration of the over-current. In this work we consider only the most conservative limit, since we want to keep a sufficient margin as we are taking decisions ahead of time with a relatively high uncertainty. The magnitude of the current  $I_l$  in link  $l$  connecting nodes  $m$  and  $n$  can be

deduced from the voltage at these nodes by

$$|I_{mn}| = \left| \left( |t_{mn}|^2 V_m - (t_{mn}^{(l)})^* t_{nm}^{(l)} V_n \right) Y_{mn}^{(br)} \right|, \quad (3)$$

where  $\cdot^*$  denotes the complex conjugate operator.

Before defining the power injections as a function of voltages, it is convenient to relate the current injected at nodes to the voltage by writing:

$$\mathbf{I} = \mathbf{YV}, \quad (4)$$

where  $\mathbf{I} = (I_1, \dots, I_{|\mathcal{N}|})$  is the vector of the current injection at nodes,  $\mathbf{V} = (V_1, \dots, V_{|\mathcal{N}|})$  is the vector of the voltage at nodes, and  $\mathbf{Y}$  is the  $|\mathcal{N}| \times |\mathcal{N}|$  nodal admittance matrix, which has its elements defined by

$$Y_{mn} = \begin{cases} -(t_{mn}^{(l)})^* t_{nm}^{(l)} Y_{mn}^{(br)} & \text{if } m \neq n \text{ and } \exists(m, n) \in \mathcal{L}, \\ \sum_{(m,k) \in \mathcal{L}} |t_{mk}|^2 (Y_{mn}^{(sh)} + Y_{mn}^{(br)}) & \text{if } m = n, \\ 0 & \text{otherwise.} \end{cases} \quad (5)$$

Regarding the active power  $P_n$  and reactive power  $Q_n$  injected at every node  $n$ , they are related to the node voltages through the power flow equations [9]:

$$\forall n \in \mathcal{N} : S_n^* = P_n - jQ_n = V_n^* I_n = V_n^* \mathbf{Y}_n V_n, \quad (6)$$

where  $S_n$  is the apparent power injection at bus  $n$  and  $\mathbf{Y}_n$  denotes the  $n^{\text{th}}$  row of the nodal admittance matrix. By convention a power injection is positive if it supplies the network and negative if it takes energy from the network.

In summary, there are four quantities attached to each node  $n \in \mathcal{N}$  that determine the electrical state of the system:  $P_n$ ,  $Q_n$ , and real and imaginary parts of  $V_n$ . The power flow equations (6) provide  $2|\mathcal{N}|$  relations.  $2|\mathcal{N}|$  variables should thus be fixed to obtain a solution to this system of equations. In general,  $V_n$  is fixed on one side of the transformer between the MV network and the transmission system, to provide a reference voltage. At other nodes, the active power injection  $P_n$  is known, as well as either the reactive power  $Q_n$  or the voltage magnitude  $|V_n|$ , depending on the type of device connected at the node. In this work we consider that we have some control over the power flows in the system, hence we consider that less than  $2|\mathcal{N}|$  variables are fixed and that we can act on  $P_n$  and  $Q_n$  at some nodes. The system is actually controlled by acting on the electrical devices attached to these nodes.

Electrical devices can be classified into two distinct subsets, the set  $\mathcal{C} \subset \mathcal{D}$  of loads that withdraw power from the network, and the set  $\mathcal{G} \subset \mathcal{D}$  of generators that inject power into the network. Within each subset, we also distinguish two types of device models. The first ones represent individual injection and withdrawal points. They can model certain types of DGs or consumers that are directly connected to the MV grid (e.g., wind farms, some companies and factories, etc.). The others model an aggregate set of devices that are assimilated to a single connection point at the MV grid (e.g., residential

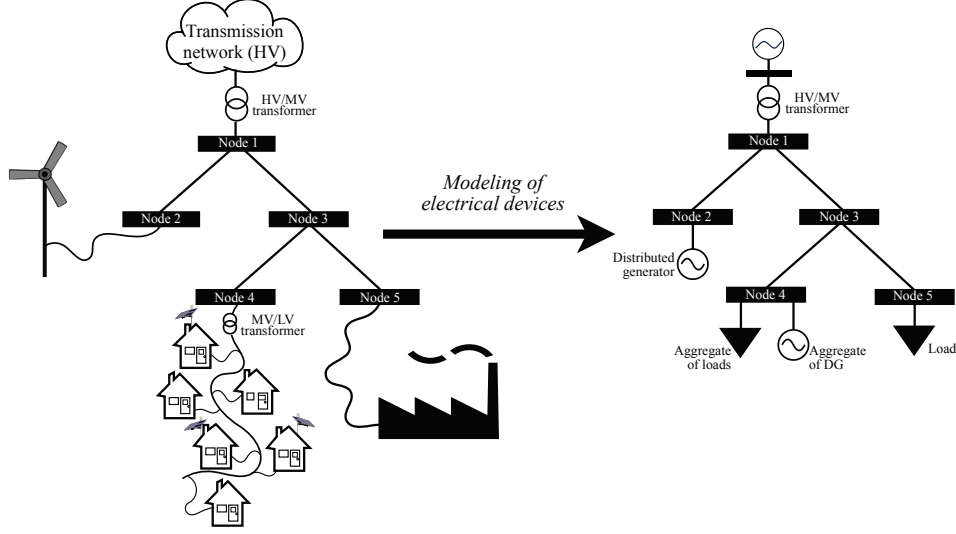


Figure 2: System model

consumers and solar panels). Correspondences between some physical elements and their device model are illustrated in Fig. 2. At node 3, a set of residential loads and a set of distributed solar units have been aggregated into a single load model and a single generator model.

An active power injection value  $P_d$  and a reactive power injection value  $Q_d$  are associated with every device  $d \in \mathcal{D}$ , and, denoting the set of devices connected at node  $n$  by  $\mathcal{D}(n) \subset \mathcal{D}$ :

$$\forall n \in \mathcal{N} : S_n = P_n + jQ_n = \sum_{d \in \mathcal{D}(n)} (P_d + jQ_d). \quad (7)$$

We also assume that all the devices are operating at a constant power factor<sup>1</sup>, so the ratio between reactive and active powers, denoted as  $\tan \phi_d$ , remains unchanged:

$$\forall d \in \mathcal{D} : \frac{Q_d}{P_d} = \tan \phi_d. \quad (8)$$

### 3.2 Operational planning problem statement

Considering the model of the electrical distribution network presented in Section 3.1, operational planning is a recurring task performed by the system operator to anticipate the evolution of the system, that is the impact of the evolution of the injection and the consumption patterns on the operational limits of the system, and take preventive decisions to stay within these limits. Among the available decisions in the considered timing of operations, we consider that acting on the power injected or consumed by

<sup>1</sup>This assumption is discussed in the conclusion.



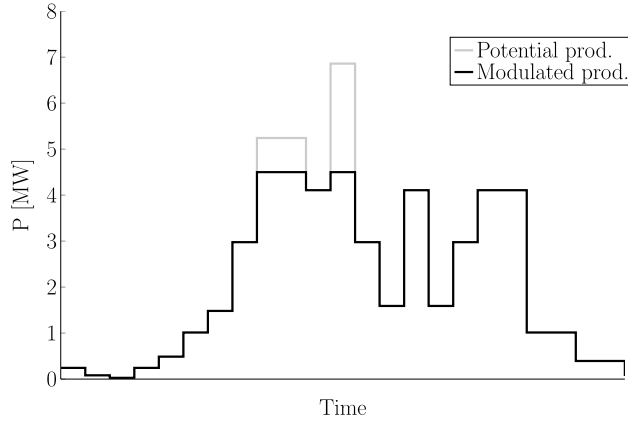
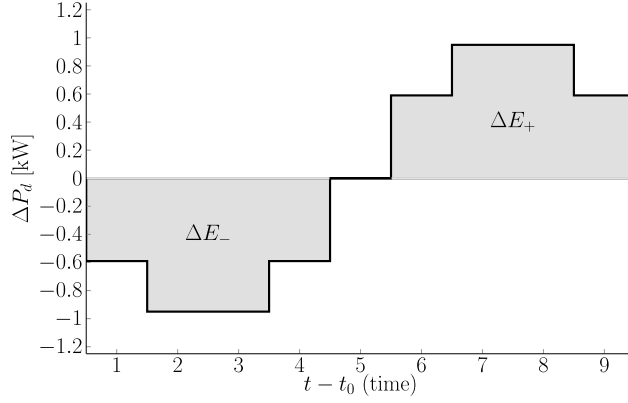


Figure 3: Curtailment of a distributed generator.

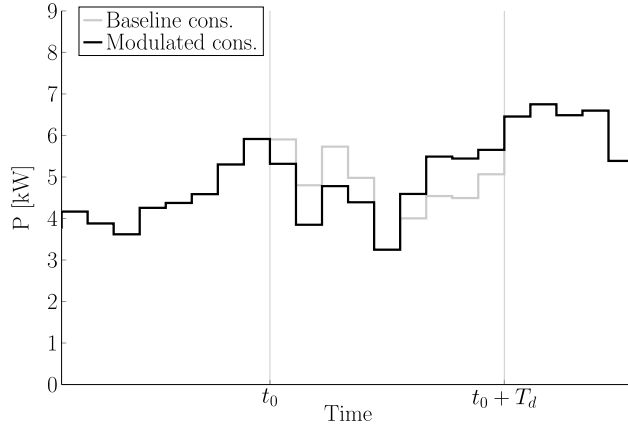
a predefined set of devices is the only type of control the DSO has, as detailed in Section 3.1. We describe the evolution of the system by a discrete-time process having a time horizon  $\mathcal{T}$ , the number of periods used for the operational planning phase. The period duration is 15 minutes, by analogy with the typical duration of a market period. The power injection and withdrawal levels are constant within a single period, and we neglect the fast dynamics of the system, which may be handled by real time controllers. The control actions in this section are aimed to directly impact these power levels and can introduce time-coupling effects, depending on the type of device. We now describe two control means of the system, the modulation of generation and the modulation of the demand, as well as one of the possible interaction schemes between the actors of this system.

We consider that the DSO can use control actions that modify the operation of the devices that are connected to its network. For each device belonging to the set  $\mathcal{G} \subset \mathcal{D}$  of DGs, it can impose a curtailment instruction, i.e. an upper limit on the production level of the DG (cf. Fig. 3). This request can be performed until the time period immediately preceding the one concerned by the curtailment and it is acquired in exchange for a fee. This fee is used to compensate the producer for financial loss related to the energy that could not be produced during modulation periods. We do not detail how this fee is set up, but we assume it is known beforehand and proportional to the energy not produced, with respect to the actual potential, that is known after the market period.

We also consider that the DSO can modify the consumption of some flexible loads. These loads constitute a subset  $\mathcal{F}$  out of the whole set of the loads  $\mathcal{C} \subset \mathcal{D}$  of the network. An activation fee is associated with this control means and flexible loads can be notified of activation until the time immediately preceding the start of the service. Once the activation is performed at time  $t_0$ , the consumption of the flexible load  $d$  is modified by a certain value during  $T_d$  periods. For each of these modulation periods  $t \in \{t_0 + 1, \dots, t_0 + T_d\}$ , this value is defined by the modulation function  $\Delta P_d(t - t_0)$ . An example of modulation function and its influence over the consumption curve are presented in Fig. 4.



(a) Modulation signal of the consumption ( $T_d = 9$ ).



(b) Impact of the modulation signal over the consumption.

Figure 4: Illustration of flexibility services.

Loads cannot be modulated in an arbitrary way. There are indeed constraints to be imposed on the modulation signal, which are inherited from the flexibility sources of the loads, such as an inner storage capacity (e.g. electric heater, refrigerator, water pump) or a process that can be scheduled with some flexibility (e.g., industrial production line, dishwasher, washing machine). In any case, we will always consider that the modulation signal  $\Delta P_d$  has to satisfy the following conditions:

- A downward modulation is followed by an increase of the consumption, and conversely.
- The integral of the modulation signal is null in order to ensure that the consumption is only shifted, not modified.

The  $\Delta P(t - t_0)$  curve of Fig. 4a respects these conditions. The modulation sign for the second part of the time interval  $\{1, \dots, T_d\}$  is opposite than it was in the first part and the

integral is null. In practice, other types of flexibility services could exist, but we restrict ourself to this definition for the sake of clarity, and because the main characteristics are already captured by the service described above.

Other approaches that we do not consider in this work exist to control the system, such as modulating the tariff signal(s), acting on the topology of the network, or using distributed storage sources. We do not model either the automatic regulation devices that often exist in distribution systems, such as On Load Tap Changers of transformers which automatically adapt to control the voltage level. This should be the case, obviously, in a real life application. We will discuss in the conclusion what are the implications of these non modeled control possibilities.

### 3.3 Optimal sequential decision making formulation

We now formalize operational planning as an optimal sequential decision making problem, that is, we explain how the time, the decision process, and uncertainty are included to extend the mathematical model described in Section 3.1. The sequentiality is induced by the modulation service that is provided by flexible loads. Indeed, if such a service is activated at time  $t_0$  for a flexible load  $d$ , the action will influence the system for the set of periods  $\{t_0 + 1, \dots, t_0 + T_d\}$ . In addition to being a sequential problem, it is also stochastic, because the evolution of the system and the outcome of control actions are affected by several uncertain factors. These factors are the wind speed, the level of solar irradiance, and the consumption level of the loads. In this section, we model this problem as a Markov decision process with mixed integer sets of states and actions. We thus consider that the transition probabilities of the stochastic elements of the system from a period  $t$  to a period  $t + 1$  only depend on the state at time  $t$ . However, this state can encompass several past values of wind speed, solar irradiance and consumption levels in order to obtain an accurate model. An automatic procedure that determine an adequate number of past values to track in the state is presented in Section 5. Finally, the notion of optimality is defined using a reward function that associates an immediate reward (or score) to every transition of the system. The better the cumulated reward over a system trajectory, the better the sequence of control actions for this trajectory.

#### 3.3.1 System state

The value of the electrical quantities can be deduced from the power injections of the devices through equations (6) and (7). If the representation of these injections requires the knowledge of the individual consumption of every load, it is possible to obtain the production of DGs given the power level of their energy source (i.e. the wind speed or the level of solar irradiance). This brings us to defining a first state set  $\mathcal{S}^{(1)}$  such that the vectors  $\mathbf{s}_t^{(1)} \in \mathcal{S}^{(1)}$  are defined by

$$\mathbf{s}_t^{(1)} = (P_{1,t}, \dots, P_{|\mathcal{C}|,t}, ir_t, v_t)$$

and contain, at time  $t \in \mathcal{T}$ , the minimal information that is required to know the power injections of the whole set  $\mathcal{D}$  of devices. The  $ir_t$  and  $v_t$  components represent the level

of solar irradiance and the wind speed, respectively. If, for the sake of simplicity, the generators that we consider are only the solar and wind ones, others could easily be integrated by increasing the dimension of  $\mathcal{S}^{(1)}$ .

Given that the DSO can influence the injection values of the devices, we introduce a second set  $\mathcal{S}^{(2)}$  that represents the modulation instructions. The vectors  $\mathbf{s}_t^{(2)} \in \mathcal{S}^{(2)}$  are defined as

$$\mathbf{s}_t^{(2)} = (\bar{P}_{1,t}, \dots, \bar{P}_{|\mathcal{G}|,t}, s_{1,t}^{(f)}, \dots, s_{|\mathcal{F}|,t}^{(f)})$$

and contain, at time  $t \in \mathcal{T}$ , the upper limits in active power injection of the DGs  $g \in \mathcal{G}$ , as authorized by the DSO, and the indicators  $s_{d,t}^{(f)}$  of the flexibility service state of the loads  $d \in \mathcal{F}$ , defined as

$$s_{d,t}^{(f)} = \begin{cases} \text{number of active periods left} & \text{if service is active} \\ 0 & \text{if service is inactive.} \end{cases}$$

We denote by  $\mathbf{s}_t^{(3)} \in \mathcal{S}^{(3)}$  the part of the system's state that, at time  $t \in \mathcal{T}$ , keeps track of past realizations of the uncertain phenomena (i.e. wind speed, solar irradiance, and consumption levels). Its purpose is solely to improve the accuracy of the stochastic model. The number of past values can be different for each phenomenon and, we have

$$\mathbf{s}_t^{(3)} = (P_{1,t-1}, \dots, P_{1,t-N_{loads}+1}, \dots, P_{|\mathcal{C}|,t-1}, \dots, P_{|\mathcal{C}|,t-N_{loads}+1}, \\ ir_{t-1}, \dots, ir_{t-N_{ir}+1}, v_{t-1}, \dots, v_{t-N_v+1})$$

where  $N_{loads}$ ,  $N_{ir}$  and  $N_v \in \mathbb{Z}_0^+$ . The value of these parameters has to be determined when instantiating the presented abstract decision model (see Section 5) and a value of 1 for any of these parameters means that the corresponding phenomenon is modeled using  $\mathbf{s}^{(1)}$  only.

Using the three sets  $\mathcal{S}^{(1)}$ ,  $\mathcal{S}^{(2)}$  and  $\mathcal{S}^{(3)}$ , we can finally define the set of states  $\mathcal{S}$  of the system as

$$\mathcal{S} = \mathcal{S}^{(1)} \times \mathcal{S}^{(2)} \times \mathcal{S}^{(3)} \times \{1, \dots, 96\},$$

where the component that belongs to the integer interval  $\{1, \dots, 96\}$  identifies the quarter of an hour in the day to which the state corresponds. This component is useful for the definition of several transition functions that rely on this information and to account that the electricity price is usually not constant during the day (see 3.3.4). In the following, we denote this component by  $q_t$ .

### 3.3.2 Control actions

The control means that are available to the DSO to control the system are modeled by the set  $\mathcal{A}_{\mathbf{s}}$  of control actions. This set depends on the state  $\mathbf{s}_t$  of the system because it is not possible to activate the flexibility service of a load if it is already active. The components of vectors  $\mathbf{a}_t \in \mathcal{A}_{\mathbf{s}}$  are defined by

$$\mathbf{a}_t = (\bar{\mathbf{p}}_t, \mathbf{a}_t^{(f)}),$$

with  $\bar{\mathbf{p}}_t \in \mathbb{R}^{|\mathcal{G}|}$  such that  $\bar{p}_{g,t}$  indicates the maximum level of active power injection for period  $t + 1$  and for each of the generators  $g \in \mathcal{G}$ . On the other hand, the vector  $\mathbf{a}_t^{(f)}$  represents the activation indicators of the flexibility services of the loads  $d \in \mathcal{F}$ , where each component  $a_{d,t}^{(f)}$  belongs to  $\mathcal{A}_{d,s}^{(f)}$ , which is defined as

$$\mathcal{A}_{d,s}^{(f)} = \begin{cases} \{0, 1\} & \text{if } s_{d,t}^{(f)} = 0 \\ \{0\} & \text{if } s_{d,t}^{(f)} > 0, \end{cases} \quad (9)$$

to ensure that a load which is already active is not activated.

By using such a representation of the control actions, we consider that a curtailment or flexibility activation action targeting a period  $t$  must always be performed at the period  $t - 1$  that precedes it. As already described in Section 3, these control actions can indeed be notified by the DSO up to the period immediately preceding their implementation. Even if it were possible to consider a model of the action vectors that integrates components implying an effective control delayed of several periods, it would induce even larger time-coupling effects, while not improving the extent of control of the DSO. Indeed, for a period  $t$ , the last recourse of the DSO is the period  $t - 1$  and the interaction model considered is such that the cost associated with an action is independent of the delay between its notification and when it becomes effective.

### 3.3.3 Transition function

The system evolution from a state  $\mathbf{s}_t$  to a state  $\mathbf{s}_{t+1}$  is described by the transition function  $f$ . The new state  $\mathbf{s}_{t+1}$  depends, in addition to the preceding state, on the control actions  $\mathbf{a}_t$  of the DSO and of the realization of the stochastic processes, modeled as Markov processes. More specifically, we have

$$f : \mathcal{S} \times \mathcal{A}_s \times \mathcal{W} \rightarrow \mathcal{S},$$

where  $\mathcal{W}$  is the set of possible realizations of a random process. The general evolution of the system is thus governed by relation

$$\mathbf{s}_{t+1} = f(\mathbf{s}_t, \mathbf{a}_t, \mathbf{w}_t), \quad (10)$$

where  $\mathbf{w}_t \in \mathcal{W}$  represents the exogenous information and such that it follows a probability law  $p_{\mathcal{W}}(\cdot)$ . We could write equivalently that  $\mathbf{s}_{t+1} \sim p_{\mathcal{S}}(\cdot | \mathbf{s}_t, \mathbf{a}_t)$ , which clearly highlights that the next state of the system follows a probability distribution that is conditional on the current state and on the action taken at the corresponding time step. However, we favor notation of equation (10) as it enables an easier formulation of concepts that are introduced latter in this paper. In order to define this function in more detail, we now describe the various elements that constitute it.

**Load consumption** The uncertainty about the behavior of consumers inevitably leads to uncertainty about the power level they draw from the network. However, over a

one-day horizon, some trends can be observed. For example, consumption peaks arise in the early morning and in the evening for residential consumers, but at levels that fluctuate from one day to another and among consumers. We model the evolution of the consumption of each load  $d \in \mathcal{C}$  by

$$P_{d,t+1} = f_d(P_{d,t}, P_{d,t-1}, \dots, P_{d,t-N_{loads}+1}, q_t, \mathbf{w}_{d,t}), \quad (11)$$

where  $\mathbf{w}_{d,t} \sim p_{\mathcal{W}_d}(\cdot)$  denotes some components of  $\mathbf{w}_t \sim p_{\mathcal{W}}(\cdot)$ . The dependency of functions  $f_d$  to the quarter of an hour in the day  $q_t$  allows for capturing the daily trends of the process. Given the hypothesis of a constant power factor for the devices, the reactive power consumption can directly be deduced from  $P_{d,t+1}$ :

$$Q_{d,t+1} = \tan \phi_d \cdot P_{d,t+1}. \quad (12)$$

In Section 5, we describe a possible procedure to model the evolution of the consumption of an aggregated set of residential consumers using relation (11).

**Speed and power level of wind generators** The uncertainty about the production level of wind turbines is inherited from the uncertainty about the wind speed. The Markov process that we consider governs the wind speed, which is assumed to be uniform across the network. The production level of the wind generators is then obtained by using a deterministic function that depends on the wind speed realization, this function is the power curve of the considered generator. We can formalize this phenomenon as:

$$v_{t+1} = f_v(v_t, \dots, v_{t-N_v+1}, q_t, \mathbf{w}_t^{(v)}), \quad (13)$$

$$P_{g,t+1} = \eta_g(v_{t+1}), \forall g \in \text{wind generators} \subset \mathcal{G}, \quad (14)$$

such that  $\mathbf{w}_t^{(v)} \sim p_{\mathcal{W}^{(v)}}(\cdot)$  denotes some components of  $\mathbf{w}_t \sim p_{\mathcal{W}}(\cdot)$  and where  $\eta_g$  is the power curve of generator  $g$ . A typical example of power curve  $\eta_g(v)$  is illustrated in Fig. 5. Like loads, the production of reactive power is obtained using:

$$Q_{g,t+1} = \tan \phi_g \cdot P_{g,t+1}. \quad (15)$$

A possible approach to determine  $f_v$ ,  $\mathcal{W}^{(v)}$ , and  $p_{\mathcal{W}^{(v)}}(\cdot)$  from a set of measurements is described in Section 5.

**Irradiance and photovoltaic production** Like wind generators, the photovoltaic generators inherit their uncertainty in production level from the uncertainty associated with their energy source. This source is represented by the level of solar irradiance, which is the power level of the incident solar energy per square meter. The irradiance level is the stochastic process that we model, while the production level is obtained by a deterministic function of the irradiance and of the surface of photovoltaic panels. This function is simpler than the power curve of wind generators and is defined as

$$P_{g,t} = \eta_g \cdot \text{surf}_g \cdot ir_t,$$

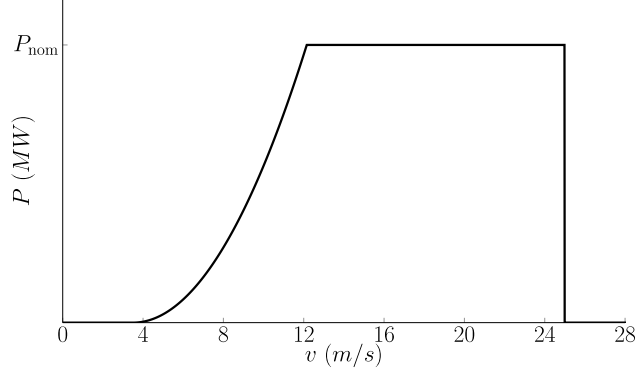


Figure 5: Power curve of a wind generator.

where  $\eta_g$  is the efficiency factor of the panels, assumed constant and with a typical value around 15%, while  $\text{surf}_g$  is the surface of the panels in  $m^2$  and is specific to each photovoltaic generator. The irradiance level is denoted by  $ir_t$  and the whole phenomenon is modeled by the following Markov process:

$$ir_{t+1} = f_{ir}(ir_t, \dots, ir_{t-N_{ir}+1}, q_t, \mathbf{w}_t^{(ir)}), \quad (16)$$

$$P_{g,t+1} = \eta_g \cdot \text{surf}_g \cdot ir_{t+1}, \forall g \in \text{solar generators} \subset \mathcal{G}, \quad (17)$$

such that  $\mathbf{w}_t^{(ir)} \sim p_{\mathcal{W}^{(ir)}}(\cdot)$  denotes some components of  $\mathbf{w}_t \sim p_{\mathcal{W}}(\cdot)$ . The technique used in Section 5 to build  $f_{ir}$ ,  $\mathcal{W}^{(ir)}$ , and  $p_{\mathcal{W}^{(ir)}}(\cdot)$  from a dataset is similar to the one for the wind speed case.

**Impact of control actions** The stochastic processes that we described govern the evolution of the state  $\mathbf{s}_t^{(1)} \in \mathcal{S}^{(1)}$  of the consumption of loads (flexibility services excluded) and of the power level of energy sources of DGs. The following transition laws now define the evolution of the components of the state of modulation instructions  $\mathbf{s}_t^{(2)} \in \mathcal{S}^{(2)}$  by integrating the control actions of the DSO:

$$\forall g \in \mathcal{G} : \quad \bar{P}_{g,t+1} = \bar{p}_{g,t}, \quad (18)$$

$$\forall d \in \mathcal{F} : \quad s_{d,t+1}^{(f)} = \max(s_{d,t}^{(f)} - 1; 0) + a_{d,t}^{(f)} T_d, \quad (19)$$

$$\forall d \in \mathcal{F} : \quad \Delta P_{d,t+1} = \begin{cases} \Delta P_d(T_d - s_{d,t+1}^{(f)} + 1) & \text{if } s_{d,t+1}^{(f)} > 0 \\ 0 & \text{if } s_{d,t+1}^{(f)} = 0. \end{cases} \quad (20)$$

From vectors  $\mathbf{s}_t^{(1)}$  and  $\mathbf{s}_t^{(2)}$ , we can determine the active and reactive power injections at nodes and thus obtain the value of the electrical quantities at nodes  $n \in \mathcal{N}$  and links

$(m, n) \in \mathcal{L}$  of the network:

$$P_{n,t} = \sum_{g \in \mathcal{G}(n)} \min(\bar{P}_{g,t}; P_{g,t}) + \sum_{d \in \mathcal{C}(n) \setminus \mathcal{F}(n)} P_{d,t} + \sum_{d \in \mathcal{F}(n)} (P_{d,t} + \Delta P_{d,t}), \quad (21)$$

$$Q_{n,t} = \sum_{g \in \mathcal{G}(n)} \min(\tan \phi_g \bar{P}_{g,t}; Q_{g,t}) + \sum_{d \in \mathcal{C}(n)} Q_{d,t} + \sum_{d \in \mathcal{F}(n)} \tan \phi_d \Delta P_{d,t}, \quad (22)$$

$$P_{n,t} - jQ_{n,t} = V_{n,t}^* \mathbf{Y}_n V_{n,t}, \quad (23)$$

$$|I_{mn,t}| = \left| \left( |t_{mn}|^2 V_{m,t} - (t_{mn}^{(l)})^* t_{nm}^{(l)} V_{n,t} \right) Y_{mn}^{(br)} \right|. \quad (24)$$

### 3.3.4 Reward function and goal

In order to evaluate the performance of a policy, we first specify the reward function  $r : \mathcal{S} \times \mathcal{A}_s \times \mathcal{S} \rightarrow \mathbb{R}$ , which associates an instantaneous reward for each transition of the system from a period  $t$  to a period  $t + 1$ :

$$\begin{aligned} r(\mathbf{s}_t, \mathbf{a}_t, \mathbf{s}_{t+1}) = & \underbrace{- \sum_{g \in \mathcal{G}} \max\{0, \frac{P_{g,t+1} - \bar{P}_{g,t+1}}{4}\} C^{curt}(q_{t+1})}_{\text{curtailment cost of DGs}} \\ & - \underbrace{\sum_{d \in \mathcal{F}} a_{d,t}^{(f)} C_d^{flex}}_{\text{activation cost of flexible loads}} - \underbrace{\Phi(\mathbf{s}_{t+1})}_{\text{barrier function}}, \end{aligned} \quad (25)$$

where  $C^{curt}(q_{t+1})$  is the curtailment price for the quarter of an hour  $q_{t+1}$  in the day and  $C_d^{flex}$  is the activation cost of the flexible loads, specific to each of them. The function  $\Phi$  is a barrier function that allows for penalizing a policy that leads the system into a state that violates the operational limits. It is defined as

$$\Phi(\mathbf{s}_{t+1}) = \sum_{n \in \mathcal{N}} [\chi(|V_{n,t+1}| - \bar{V}_n) + \chi(V_n - |V_{n,t+1}|)] + \sum_{l \in \mathcal{L}} \chi(|I_{l,t+1}| - \bar{I}_l), \quad (26)$$

where  $|V_{n,t+1}|$  ( $n \in \mathcal{N}$ ) and  $I_{l,t+1}$  ( $l \in \mathcal{L}$ ) are determined from  $\mathbf{s}_{t+1}$  using equations (21)-(24) and

$$\chi(x) = \begin{cases} 10^3 \min(\exp(x) - 1, 10^3) & \text{if } x > 0 \\ 0 & \text{otherwise.} \end{cases} \quad (27)$$

The higher the operational costs and the larger the violations of operational limits, the more negative the reward function.

We can now define the *return over  $T$  periods*, denoted  $R_T$ , as the weighted sum of the rewards that are observed over a system trajectory of  $T$  periods

$$R_T = \sum_{t=0}^{T-1} \gamma^t r(\mathbf{s}_t, \mathbf{a}_t, \mathbf{s}_{t+1}), \quad (28)$$



where  $\gamma \in ]0; 1[$  is the discount factor. Given that  $\gamma^t < 1$  for  $t > 0$ , the further in time the transition from period  $t = 0$ , the less importance is given to the associated reward. Because the operation of a DN must always be ensured, it does not seem relevant to consider returns over a finite number of periods and we introduce the *return*  $R$  as

$$R = R_\infty = \lim_{T \rightarrow \infty} \sum_{t=0}^{T-1} \gamma^t r(\mathbf{s}_t, \mathbf{a}_t, \mathbf{s}_{t+1}), \quad (29)$$

that corresponds to the weighted sum of the rewards observed over an infinite trajectory of the system. Given that the costs and penalties have finite values and that the reward function  $r$  is the sum of an infinite number of these costs and penalties, a constant  $C$  exists such that,  $\forall (\mathbf{s}_t, \mathbf{a}_t, \mathbf{s}_{t+1}) \in \mathcal{S} \times \mathcal{A}_s \times \mathcal{S}$ , we have  $|r(\mathbf{s}_t, \mathbf{a}_t, \mathbf{s}_{t+1})| < C$  and thus

$$|R| < \lim_{T \rightarrow \infty} C \sum_{t=0}^{T-1} \gamma^t = \frac{C}{1 - \gamma}. \quad (30)$$

It means that even if the return  $R$  is defined as an infinite sum, it converges to a finite value. One can also observe that, because  $\mathbf{s}_{t+1} = f(\mathbf{s}_t, \mathbf{a}_t, \mathbf{w}_t)$ , a function  $\rho : \mathcal{S} \times \mathcal{A} \times \mathcal{W} \rightarrow \mathbb{R}$  exists that aggregates functions  $f$  and  $r$  such that

$$\rho(\mathbf{s}_t, \mathbf{a}_t, \mathbf{w}_t) = r(\mathbf{s}_t, \mathbf{a}_t, f(\mathbf{s}_t, \mathbf{a}_t, \mathbf{w}_t)) = r(\mathbf{s}_t, \mathbf{a}_t, \mathbf{s}_{t+1}), \quad (31)$$

with  $\mathbf{w}_t \sim p_{\mathcal{W}}(\cdot)$ . Let  $\pi : \mathcal{S} \rightarrow \mathcal{A}_s$  be a policy that associates a control action to each state of the system. We can define, starting from an initial state  $\mathbf{s}_0 = \mathbf{s}$ , the expected return  $R$  of the policy  $\pi$  by

$$J^\pi(\mathbf{s}) = \lim_{T \rightarrow \infty} \mathbb{E}_{\substack{\mathbf{w}_t \sim p_{\mathcal{W}}(\cdot) \\ t=0,1,\dots}} \left\{ \sum_{t=0}^{T-1} \gamma^t \rho(\mathbf{s}_t, \pi(\mathbf{s}_t), \mathbf{w}_t) \mid \mathbf{s}_0 = \mathbf{s} \right\}. \quad (32)$$

We denote by  $\Pi$  the space of all the policies  $\pi$ . For a DSO, addressing the operational planning problem described in Section 3 is equivalent to determine an optimal policy  $\pi^*$  among all the elements of  $\Pi$ , i.e. a policy that satisfies the following condition

$$J^{\pi^*}(\mathbf{s}) \geq J^\pi(\mathbf{s}), \forall \mathbf{s} \in \mathcal{S}, \forall \pi \in \Pi. \quad (33)$$

It is well known that such a policy satisfies the Bellman equation [10], which can be written

$$J^{\pi^*}(\mathbf{s}) = \max_{\mathbf{a} \in \mathcal{A}_s} \mathbb{E}_{\mathbf{w} \sim p_{\mathcal{W}}(\cdot)} \{ \rho(\mathbf{s}, \mathbf{a}, \mathbf{w}) + \gamma J^{\pi^*}(f(\mathbf{s}, \mathbf{a}, \mathbf{w})) \}, \forall \mathbf{s} \in \mathcal{S}. \quad (34)$$

If we only take into account the space of stationary policies (i.e. that selects an action independently of time  $t$ ), it is without loss of generality comparing to the space of policies  $\Pi' : \mathcal{S} \times \mathcal{T} \rightarrow \mathcal{A}$  because the return to be maximized corresponds to an infinite trajectory of the system [11].

## 4 Formulating operational planning as a MINLP

We now describe a look-ahead algorithm to build a policy based on stochastic programming. The principle is, at each time step  $t \in \mathcal{T}$ , to optimize a model  $\mathcal{M}_t$  of the system over a finite time horizon  $\mathcal{T}_t = \{t, \dots, t + T - 1\}$  and to apply the control action  $\hat{\mathbf{a}}_t^* = \hat{\pi}_{\mathcal{M}_t}^*(\mathbf{s}_t)$  that corresponds to the first stage of the model. This approximate optimal policy  $\hat{\pi}_{\mathcal{M}_t}^*$  can be formalized as

$$\hat{\pi}_{\mathcal{M}_t}^*(\mathbf{s}_t) = \arg \max_{\mathbf{a}_t} \max_{\substack{\mathbf{s}_{t'}, \mathbf{a}_{t'} \\ \forall t' \in \mathcal{T}_t}} \mathbb{E}_{\mathbf{w}_{t'} \sim p_{\mathcal{W}}(\cdot)} \left[ \sum_{t'=t}^{t+T-1} \gamma^{t'-t} r(\mathbf{s}_{t'}, \mathbf{a}_{t'}, f(\mathbf{s}_{t'}, \mathbf{a}_{t'}, \mathbf{w}_{t'})) \right] \quad (35)$$

$$\text{s.t.} \quad \mathbf{s}_{t'} = f(\mathbf{s}_{t'-1}, \mathbf{a}_{t'-1}, \mathbf{w}_{t'-1}), \quad \forall t' \in \mathcal{T}_t \setminus \{t\} \quad (36)$$

$$\mathbf{a}_{t'} \in \mathcal{A}_{\mathbf{s}_{t'}}, \quad \forall t' \in \mathcal{T}_t, \quad (37)$$

where the shorter the horizon  $T$ , the higher the approximation error. However, it is not the only source of approximation. First, there is no exact numerical method to solve (35)-(37) without requiring a discrete approximation of the continuous stochastic processes [12]. Then, because of the non-linearity of power-flow equations on the one hand, and the integer variables that model the activation of flexibility services on the other hand, the resulting mathematical problem is very complex to solve. For this reason, it is often required to resort to local optimization techniques and to heuristics.

The next step toward a policy that can be implemented by a computer program is to discretize the random process over the look-ahead horizon. A prevalent technique is to use a scenario tree [13] for this purpose. At each time step  $t \in \mathcal{T}$ , the evolution of the stochastic components is aggregated as a finite set  $\tilde{\mathcal{W}}_t^T$  of outcome trajectories of the exogenous variables:

$$\tilde{\mathcal{W}}_t^T = \{(\mathbf{w}_t^{(k)}, \dots, \mathbf{w}_{t+T-1}^{(k)}) | k = 1, \dots, W\}, \quad (38)$$

and a probability  $\mathbb{P}_k$  is associated to each trajectory  $k \in \{1, \dots, W\}$ . If two trajectories  $i$  and  $j$  share the same outcomes up to stage  $o$ , i.e. if  $(\mathbf{w}_{t'}^{(i)}, \dots, \mathbf{w}_{t'+o}^{(i)}) = (\mathbf{w}_{t'}^{(j)}, \dots, \mathbf{w}_{t'+o}^{(j)})$ , they can be interpreted as a single trajectory of probability  $\mathbb{P}_i + \mathbb{P}_j$  up this stage. Fig. 6 provides an example of such a scenario tree, where the nodes represent the outcomes and the edges correspond to the transition probabilities. Another computational obstacle is the form of equation (25), i.e. the reward function, and, in particular, of the barrier term defined by equations (26) and (27). This term should appear in the objective function of problem (35)-(37) but it is not straightforward to implement it in a mathematical program. We chose to remove these terms and to approximate them by forbidding the policy to bring the state of the look-ahead model where equation (26) is different than zero. This is implemented by adding constraints to (35)-(37) that correspond to the operational constraints defined in equations (1) and (2). The new objective function



nonanticipativity constraints [12] to the mathematical program using equation (42). Finally, problem (41)-(46) falls within the class of mixed integer non-linear programs (MINLP) upon the following arrangements:

- $\max(x, y)$  and piecewise functions in equations (9),(19),(21),(22), and (40) are implemented using a *big M* formulation [14];
- modulation signals of flexible loads described in equation (20) are modeled by

$$\Delta P_{d,t'+1} = \sum_{\tau=t}^{t'} a_{d,\tau}^{(f)} \Delta P_d(t' - \tau) \quad (47)$$

for the activations that occurs over the lookahead horizon, which enables to exclude the definition of  $\Delta P_d$  functions from (41)-(46) and to consider the modulation signals as series of parameters by computing  $\Delta P_d(t' - \tau)$  values before solving the mathematical program.

## 5 Test instance

In this section, we describe a test instance of the considered problem. The set of models and parameters that are specific to this instance, as well as documentation for their usage, are accessible at <http://www.montefiore.ulg.ac.be/~anm/> as Python code. It has been developed to provide a black-box-type simulator that is quick to set up. The DN on which this instance is based is a generic DN of 75 buses [15] that has a radial topology, which is presented in Fig. 7. We bound various electrical devices to the network in such a way that it is possible to gather the nodes of this network into four distinct categories:

- each *residential* node is the connection point of a load that represents a set of residential consumers and of a generator that models the photovoltaic installations that are on the roofs on the houses;
- each *production* node allows the connection of a wind generator that has a capacity of 6 MW;
- *topological* nodes do not correspond to devices, but serve the topology by creating ramifications in the network;
- the *slack* node models the TN as seen from the DN; it guarantees the balance between the consumed and produced powers within the network and a constant voltage magnitude and zero angle is associated to this node, so that it serves as a reference.

The sizing of the devices is such that the overall load consumption of the 53 residential nodes peaks close to 20 MW, while the photovoltaic installations represent a total surface of 98,610  $m^2$  with an efficiency of 20%.

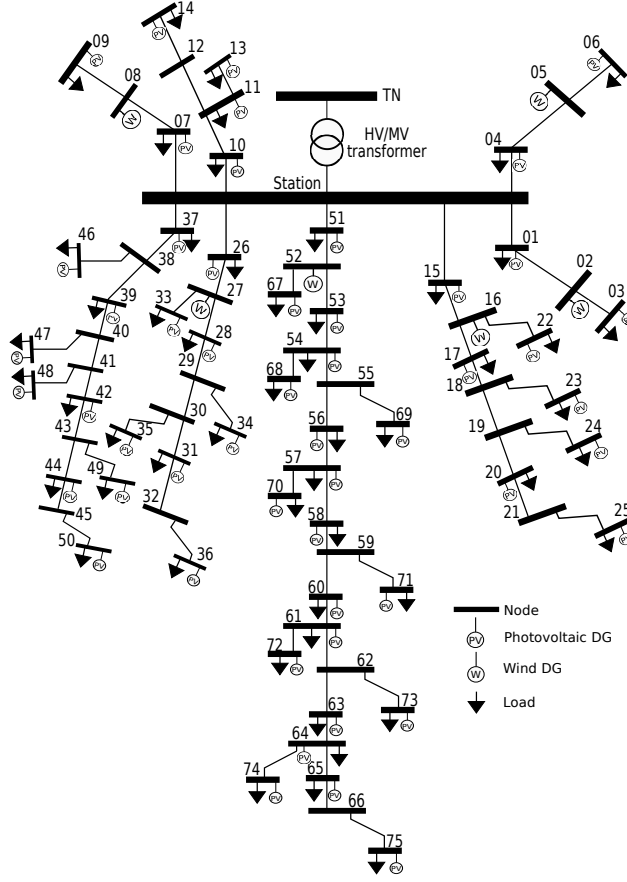


Figure 7: Test network.

We assume that the curtailment actions can be applied to wind generators, at a cost that is defined in Section 3.3.4. Concerning the flexible loads, we define their modulation signal,  $\forall d \in \mathcal{F}$ , as

$$\Delta P_d(t_d) = \begin{cases} \pm \Delta_d \sin(1.8\pi \frac{t_d - 0.5(T_d + 1)}{T_d - 1}) & \text{if } \forall t_d \in \{1, \dots, T_d\} \\ 0 & \text{otherwise} \end{cases} \quad (48)$$

where the sign of  $\Delta P_d(t')$  depends on the type of modulation that is offered by the load  $d$  (i.e. upward or downward). We account for three different penetration levels of flexibility services, which yield three specializations of the instance (see Table 1). About half of the loads offer a downward modulation, followed by an upward rebound effect, and inversely for the other half. These flexibility services are illustrated in Fig. 8. Parameters  $\Delta_d$  and  $T_d$  are specific to each load and we consider that the activation costs are proportional to the magnitude of the modulation signals ( $C_d^{flex} \propto \Delta_d$ ).

The approach used to build the transition functions (11), (13), and (16), of the stochastic quantities (i.e. the consumption of the loads, the wind speed, and the level

Table 1: Number of flexible loads and maximum of sum modulation signals for each penetration level.

Name	$ \mathcal{F} $	$\sum_{d \in \mathcal{F}} \max_{1 \leq t \leq T_d} \Delta P_d(t)$
Low	11	1.7 MW
Medium	22	3.4 MW
High	33	5.0 MW

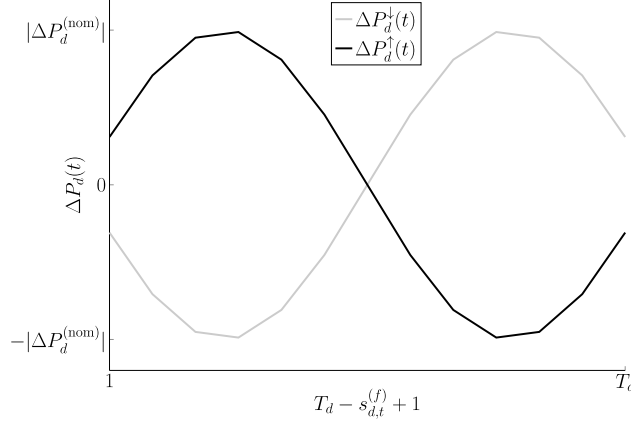


Figure 8: Modulation signal models used in the test instance.

of solar irradiance) is to learn the parameters of a Markov process model from time series of measurements. The considered parametric model  $\mathcal{P}_{(N,n)}$  relies on a mixture of  $n$  Gaussians to represent the probability distribution  $p(x_{t+1}|x_t, \dots, x_{t-N+1})$  of the next outcome of the process, conditionally to the last  $N$  observed outcomes. In particular, the following procedure allows to fit a model  $\mathcal{P}_{(N,n)}$  to a set  $\{(x_1^{(i)}, x_2^{(i)}, \dots, x_L^{(i)}), i = 1, \dots, I\}$  of time series :

1. build a dataset of tuples  $(x_{t-N+1}^{(i)}, \dots, x_t^{(i)}, x_{t+1}^{(i)}), \forall (i, t) \in \{1, \dots, I\} \times \{N, \dots, L-1\}$ ;
2. model the joint distribution  $p(x_{t-N+1}, \dots, x_{t+1})$  of the dataset using a mixture of  $n$  Gaussians, by performing a maximum likelihood estimation [16] of the mixture's parameters (i.e. the weight  $\eta_i$ , mean  $\mathbf{w}_i$ , and covariance matrix  $\mathbf{\Sigma}_i$  of every Gaussian  $i \in \{1, \dots, n\}$ );
3.  $\forall i \in \{1, \dots, n\}$ , deduce from  $\mathbf{w}_i$  and  $\mathbf{\Sigma}_i$  the functions  $\mu_i(x_{t-N+1}, \dots, x_{t-1})$  and  $\sigma_i(x_{t-N+1}, \dots, x_{t-1})$  that define the mean and standard deviation of  $x_{t+1}$ , according to the  $i^{\text{th}}$  Gaussian in the mixture and conditional to  $x_{t-N+1}, \dots, x_t$  [17].

Table 2: Parameters of the stochastic models used in the implementation of the benchmark.

	$N$	$n$
Wind speed ( $N_v$ )	1	1
Solar irradiance ( $N_{ir}$ )	1	10
Load consumption ( $N_{loads}$ )	2	10

Denoting by  $x_t$  any of the state variables  $P_{d,t}$ ,  $v_t$ , or  $ir_t$ , this procedure produces a transition function that takes the form

$$x_t = f(x_{t-1}, \dots, x_{t-N}, w_1, w_2) \quad (49)$$

$$= \begin{cases} \mu_1(x_{t-1}, \dots, x_{t-N}) + w_2 \sigma_1(x_t, \dots, x_{t-N}) & \text{if } w_1 < \eta_1, \\ \dots & \\ \mu_i(x_{t-1}, \dots, x_{t-N}) + w_2 \sigma_i(x_t, \dots, x_{t-N}) & \text{if } \sum_{j=1}^{i-1} \eta_j \leq w_1 < \sum_{j=1}^i \eta_j, \\ \dots & \\ \mu_n(x_{t-1}, \dots, x_{t-N}) + w_2 \sigma_n(x_t, \dots, x_{t-N}) & \text{if } \sum_{j=1}^{n-1} \eta_j \leq w_1, \end{cases} \quad (50)$$

with  $(w_1, w_2) \sim \mathcal{U}(0, 1) \times \mathcal{N}(0, 1)$ .

In order to determine an adequate value of the model's parameters  $n$  and  $N$  for each process, we relied on an Approximate Bayesian Computation (ABC) method [18]. Such an approach consists in sampling trajectories from each model and to compare them with the original data to estimate its posterior probability among the set  $\Theta$  of candidate models [19]. Using  $\Theta = \{\mathcal{P}_{(N,m)} | n \in \{1, \dots, 20\}, N \in \{1, \dots, 3\}\}$ , the most likely parameters identified by this model choice technique are presented in Table 2.

The datasets that we used are real measurements of the wind speed<sup>2</sup> and of the solar irradiance<sup>3</sup>. For the residential consumption data, a single stochastic model has been learned from measurements of a Belgian distribution network and is used for all the loads of the test instance. However, this model differs among the loads through the use of a scaling factor. The implementation of the statistical algorithms relies on both SciPy [20] and Scikit-learn [21], two Python libraries.

## 6 Numerical results

The goal of this section is twofold: to illustrate the operational planning problem and the test instance of Section 5 and to assess the performance of the proposed solution technique. In particular, the policy  $\hat{\pi}_{\mathcal{M}_t}^*(s_t)$  defined by problem (41)-(46) was applied to the test instance for 50 runs of 288 time steps (i.e. of 3 days) each run  $i$  corresponding to the following sequence:

<sup>2</sup>[http://www.nrel.gov/electricity/transmission/eastern\\_wind\\_dataset.html](http://www.nrel.gov/electricity/transmission/eastern_wind_dataset.html)

<sup>3</sup><http://solargis.info/>

1. Initialize the state vector  $\mathbf{s}_0$  by setting all the flexible loads as inactive and by sampling stochastic components from the joint distributions learned when building the test instance.
2. Run a simulation of 288 time steps, where, at every time step, problem (41)-(46) is implemented as follow:
  - (a) sample 100 trajectories of the exogenous variables over a lookahead horizon of length  $T = 15$ , i.e. trajectories  $(\mathbf{w}_t^{(j)}, \dots, \mathbf{w}_{t+14}^{(j)})$ , with  $j = 1, \dots, 100$ ;
  - (b) determine the corresponding trajectories of the power injections of the devices, as they are fully determined by the current state  $\mathbf{s}_t$  and by  $(\mathbf{w}_t^{(j)}, \dots, \mathbf{w}_{t+14}^{(j)})$ ;
  - (c) cluster the 100 trajectories of power injections into  $W$  scenarios, using a hierarchical clustering method and Ward's distance [22];
  - (d) build the corresponding clusters of outcome trajectories, i.e.

$$\tilde{\mathcal{W}}_t^T = \{(\tilde{\mathbf{w}}_t^{(k)}, \dots, \tilde{\mathbf{w}}_{t+14}^{(k)}) | k = 1, \dots, W\},$$

where  $\tilde{\mathbf{w}}_{t'}^{(k)}$  denotes the centroid of cluster  $k$  at time  $t' \in \{t, \dots, t+14\}$ , and compute the probabilities  $\mathbb{P}_k$  of the resulting scenarios as

$$\mathbb{P}_k = \frac{\text{number of trajectories in cluster } k}{100};$$

- (e) solve the MINLP problem  $\hat{\mathcal{M}}_t$  with a discount factor  $\gamma = 0.99$  and over the scenario tree defined by outcomes of  $\tilde{\mathcal{W}}_t^T$  and probabilities  $(\mathbb{P}_1, \dots, \mathbb{P}_W)$ , using a branch and bound algorithm [23] for integer variables and an interior-point method [24] for continuous relaxations;
- (f) recover the action vector  $\mathbf{a}_t$  to apply to the system, upon the following processing of the solution for curtailment decisions:

$$\forall g \in \mathcal{G} : \bar{p}_{g,t} \leftarrow \begin{cases} \bar{p}_{g,t} & \text{if } \exists k \in \{1, \dots, W\} \text{ s.t. } \bar{p}_g < P_{g,t+1}^{(k)}, \\ +\infty & \text{otherwise,} \end{cases} \quad (51)$$

where  $P_{g,t+1}^{(k)}$  denotes the power injection of generator  $g$  at the next time period, according to scenario  $k$ .

The motivation behind the use of Ward's method to cluster trajectories is that it is a minimum variance method, which means that the trajectories of a cluster were selected because they are close to its centroid, in comparison to trajectories of other clusters. Consequently, the scenarios used in the optimization model, which are the centroids of the clusters, differ minimally from the trajectories it summarizes. The processing of curtailment decisions described at step (2f) was introduced because, in the mathematical program  $\hat{\mathcal{M}}_t$ , the value of variables  $\bar{p}_{g,t}$  has no meaning when it does not induce an actual curtailment for at least one scenario. Therefore, it makes no sense to



interpret these variables as curtailment instructions and equation (51) makes sure that curtailment actions sent to the system actually corresponds to curtailment decisions in the optimization model.

The implementation has been done using the Python code mentioned in Section 5 to simulate the system, Pyomo [25] to build the mathematical programs and BONMIN [26] to solve them. If BONMIN is not able to find a feasible solution within ten minutes, a fallback optimization problem that only considers curtailment actions for the next time period, i.e. a much simpler problem, is solved. For each flexibility level of the test instance, the same runs were performed with a scenario tree  $\tilde{\mathcal{W}}_t^T$  of one scenario (i.e. the mean of the sampled trajectories) and of three scenarios. A version of the problem with perfect information, i.e. with a scenario tree consisting of the actual future trajectory of the exogenous information, was also simulated to obtain a reference value of performance. The overall simulation was carried on in a cloud computing environment, on a virtual machine of 32 cores. Each run being limited to a single core, such an infrastructure enabled 32 simulations to run in parallel and thus to speed up computations by the same factor. The empirical estimations of the expected return reported in the following results are computed as:

$$\mathbb{E}_{\mathbf{s} \sim p_0(\cdot)} \left\{ J^{\hat{\pi}^*}(\mathbf{s}) \right\} \approx \frac{1}{50} \sum_{i=1}^{50} \sum_{t=0}^{287} 0.99^t r_t^{(i)}, \quad (52)$$

where  $r_t^{(i)}$  corresponds to the instantaneous reward observed during the  $i^{\text{th}}$  simulation run at time step  $t$ , and where  $p_0(\cdot)$  denotes the probability distribution described at step (1).

Fig. 9 and Fig. 10 illustrate the solutions obtained using the simulator of the benchmark. Fig. 9 defines the content of all the subplots while Fig. 10 compares the deterministic setting to the stochastic setting. Fig. 11 shows the estimation of the expected return versus the mean solver time for the nine trials considered. This plot highlights that having a perfect forecast of the evolution of the system yields significantly lower operation costs than when decisions are subject to uncertainty. It also shows that considering three possible future scenarios can significantly improve over an optimization performed on the average future scenario. However, the solution time is significantly impacted. We also observe that the policy benefits from an increase of the flexibility level of loads in the deterministic setting, while it is not the case in the stochastic configuration. This observation being more evident when the lookahead model uses three scenarios, we suspect that this is induced by the optimality of the solver’s solutions, which deteriorates as the complexity of the mathematical program  $\hat{\mathcal{M}}_t$  increases. Fig. 12 gives more insight on the solution time distribution, and confirms that optimizing over the average scenario is faster than on a deterministic scenario. This suggests that aggregating scenarios in the scenario tree should be done more carefully, since a lot of information seems lost in this process and makes the problem easier to solve. Finally, we reports in Table (3) some figures that describe the simulation runs.

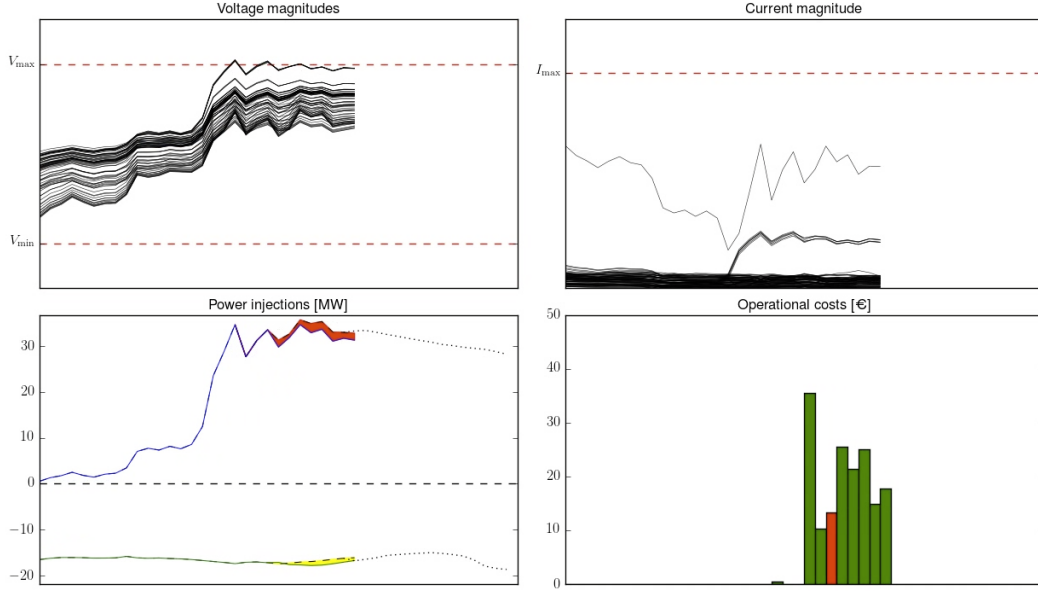
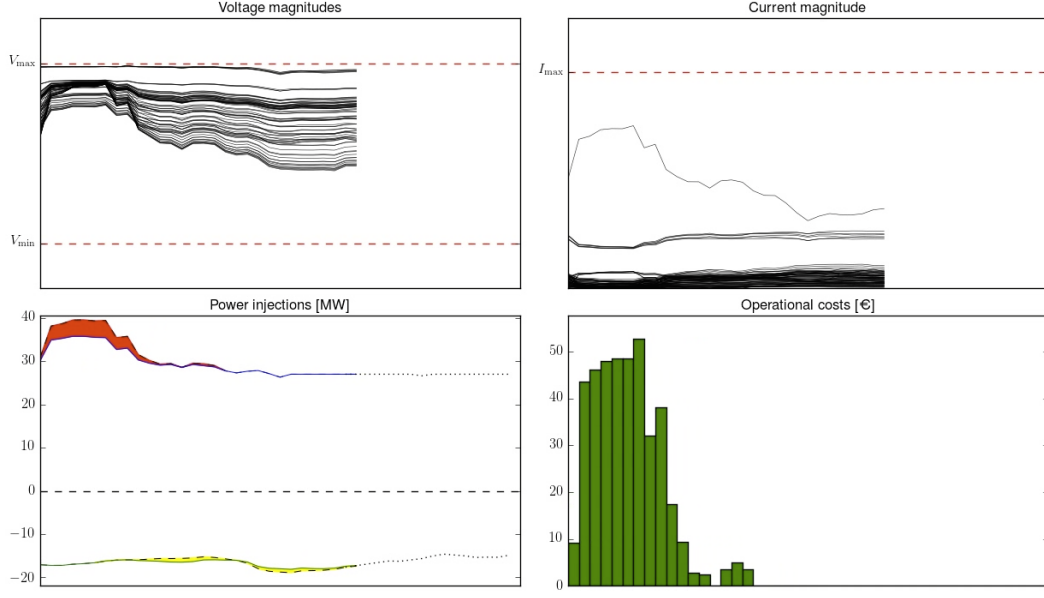


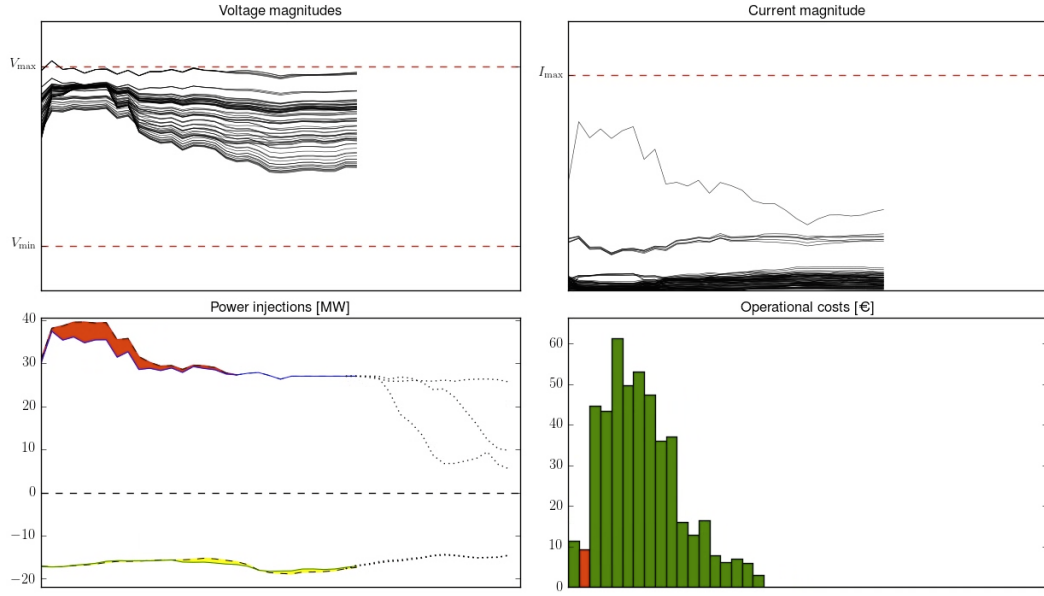
Figure 9: Screen captures of the simulator. On all subplots the horizontal axis represents time. Time indices are not shown, but the curves actually stop at the present time, and the remainder of the horizon used for optimization is shown. Top left: evolution of normalized voltage magnitudes at all the buses, dashed lines represent the lower and upper voltage limits. Top right: evolution of the normalized current in the links, dashed lines represent the current limit. Bottom left: Evolution of the total injection (above zero) and total withdrawal (below zero), with curtailed generation in red and shifted consumption in yellow. The dotted lines extending these curves represent the forecasted values, which usually differ from the realized values. Bottom right: instantaneous cost, the bar is red when an operational limit is exceeded. Optimization on the average scenario with high flexibility.

Table 3: Figures summarizing the behavior of policy  $\hat{\pi}_{\mathcal{M}_t}^*$  over the simulation runs.

Configuration	Flexibility level	$\mathbb{E}(J^{\hat{\pi}})$	Periods with violations (%)	Recourses to fallback policy (%)
Deterministic	low	-460.2	0	0.11
	medium	-453.6	0	0.44
	high	-451.5	0	0.67
1 scenario	low	-727.1	2.04	0.09
	medium	-731.5	2.08	0.33
	high	-727.2	2.1	0.52
3 scenarios	low	-649.1	1.6	0.43
	medium	-647.8	1.87	1.1
	high	-697.8	1.86	1.6



(a) Optimization with perfect knowledge of the future.



(b) Optimization based on three scenarios.

Figure 10: Comparison of decisions taken as a function of the uncertainty level on two simulations performed with the same seed. The subplots represent the same information as in Fig. 9. From both cases, it can be observed that the policy uses flexibility only when the excess generation is forecasted to last less than half of the modulation signal of flexible loads, since it wants to avoid worsening the situation when loads compensate the over-consumption. Decisions never lead to a violation of operational limits in the deterministic case and one of the voltages stays very close to the limit, whereas a violation occurs in the stochastic case by lack of curtailment, as indicated by the little red bar in the bottom right plot of Fig. 10b.

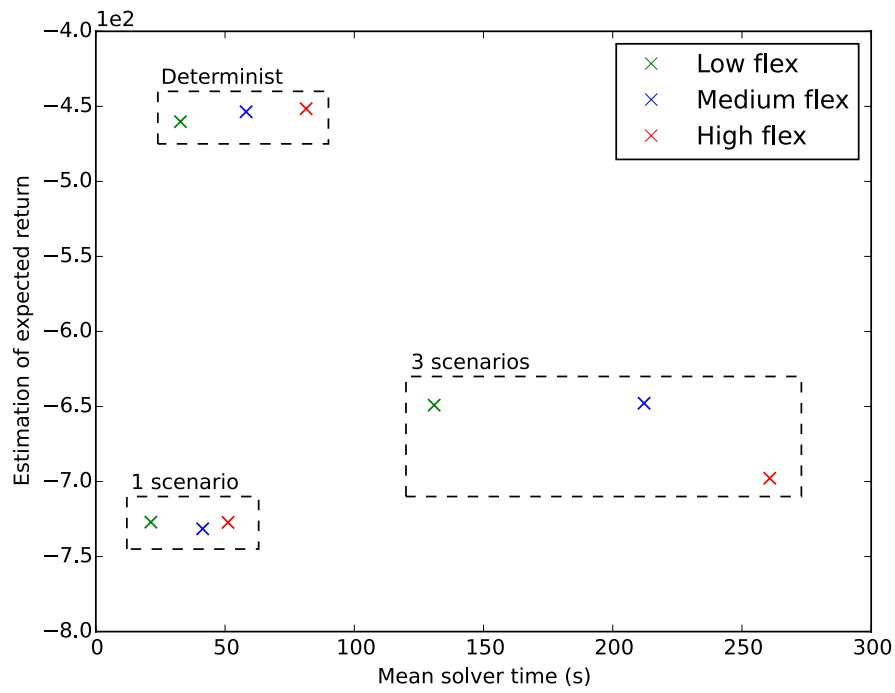


Figure 11: Estimation of expected return vs. mean solver time for the nine trials considered.

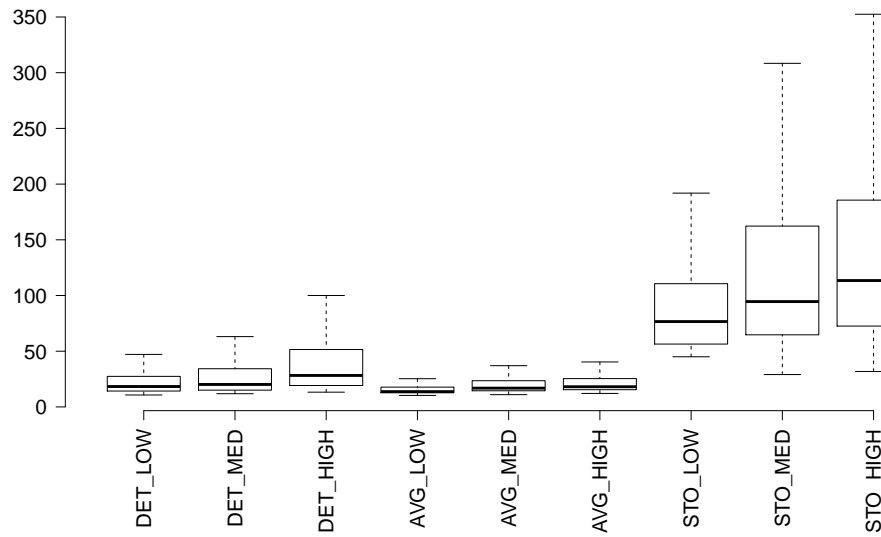


Figure 12: Distribution of MINLP solution time in seconds. Outliers are not shown, but few sessions take significantly more time than the maximum value shown on the plot.

## 7 Conclusions

Active Network Management is an alternative or a complement to network reinforcement in case of massive integration of renewable energy in distribution systems in the future. Mathematically, operational planning, which is the preventive version of active network management we consider in this paper, is an optimal sequential decision making problem under uncertainty. The properties of the operational planning problem that we want to highlight are the need to optimize over a sufficiently long time horizon, to account for uncertainty of generation and consumption, and to model the discrete decisions related to the activation of flexibility services. In an attempt not to restrict ourselves to one solution method and one research community, we provide a formulation of this problem as a Markov Decision Process (MDP), which does not call for a particular solution method. We provide a benchmark at <http://www.montefiore.ulg.ac.be/~anm/> along with this formulation to foster research in this field, and ease future comparison of results. Although the benchmark is not taken from a real system, its size and properties are coherent with what system operators could face in real life. We detail one possible solution method, which is Mixed Integer Non-Linear Programming, then cast the MDP as a sequence of MINLPs and provide results on the benchmark we created. Results show that state of the art open source local solvers for MINLP can actually show good performance on this problem, at least when we approximate the stochastic program with few scenarios. On the modeling side, we considered that all buses except the slack bus are P-Q buses, and that the power factors of the devices are constant. Possible extensions of this work could be to consider the control of steerable synchronous generation, and the control of  $Q$  of some devices that can operate with  $P$  and  $Q$  that lie in a feasible space that does not boil down to a single point, as wind turbines for instance. As mentioned in Section 3.2, other approaches exist to control the system, such as modulating the tariff signal(s), acting on the topology of the network, or using distributed storage sources. We did not model either the automatic regulation devices that often exist in distribution systems, such as On Load Tap Changers (OLTCs) of transformers that automatically adapt to control the voltage level. These aspects should be considered in a real life solution. However, computational experiments show that we are at the limit of what can be achieved with modern computers and standard MINLP tools. Furthermore including a more detailed representation of the physical system makes the problem yet more non-linear (e.g. control over  $Q$ ), more discrete (OLTCs), and more uncertain (for instance, if flexibility services are not as well characterized as what we have assumed). Our experiments also show that increasing the number of scenarios, or stages of the stochastic program, would probably significantly improve the policies. All these observations suggest further research for tailored approximation or decomposition techniques, for instance techniques relying on the dynamic programming framework, in particular *approximate dynamic programming*, or simulation methods, such as *direct policy search* [27] or *Monte-Carlo tree search* [28, 29], or other approaches from the robust and stochastic programming community [30]. Actually the benchmark that we proposed makes the comparison of new techniques possible.

## Acknowledgements

This research is supported by the public service of Wallonia - Department of Energy and Sustainable Building within the framework of the GREDOR project. The authors give their thanks for the financial support of the Belgian Network DYSCO, an Inter-university Attraction Poles Program initiated by the Belgian State, Science Policy Office. The authors would also like to thank Raphaël Fonteneau and Mevludin Glavic for their precious advices and comments.

## References

- [1] D. Fouquet and T.B. Johansson. European renewable energy policy at crossroads – focus on electricity support mechanisms. *Energy Policy*, 36(11):4079–4092, 2008.
- [2] J.A.P. Lopes, N. Hatziaargyriou, J. Mutale, P. Djapic, and N. Jenkins. Integrating distributed generation into electric power systems: A review of drivers, challenges and opportunities. *Electric Power Systems Research*, 77(9):1189–1203, 2007.
- [3] S.N. Liew and G. Strbac. Maximising penetration of wind generation in existing distribution networks. *IET Generation Transmission and Distribution*, 149(3):256–262, 2002.
- [4] L.F. Ochoa, C.J. Dent, and G.P. Harrison. Distribution network capacity assessment: Variable DG and active networks. *IEEE Transactions on Power Systems*, 25(1):87–95, 2010.
- [5] M. J. Dolan, E. M. Davidson, I. Kockar, G. W. Ault, and S. D. J. McArthur. Distribution power flow management utilizing an online optimal power flow technique. *IEEE Transactions on Power Systems*, 27(2):790–799, 2012.
- [6] Q. Gemine, E. Karangelos, D. Ernst, and B. Cornélusse. Active network management: planning under uncertainty for exploiting load modulation. In *Proceedings of the 2013 IREP Symposium - Bulk Power System Dynamics and Control - IX*, page 9, 2013.
- [7] H.W. Dommel and W.F. Tinney. Optimal power flow solutions. *IEEE transactions on Power Apparatus and Systems*, PAS-87(10):1866–1876, 1968.
- [8] G. Andersson. Modelling and analysis of electric power systems. *EEH-Power Systems Laboratory, Swiss Federal Institute of Technology (ETH), Zürich, Switzerland*, 2004.
- [9] A. Monticelli. *State estimation in electric power systems: a generalized approach*, volume 507. Springer Science & Business Media, 1999.
- [10] R. Bellman. *Dynamic Programming*. Princeton University Press, 1957.

- [11] D.P. Bertsekas and S.E. Shreve. *Stochastic Optimal Control: The Discrete Time Case*. Academic Press New York, 1978.
- [12] A. Shapiro, D. Dentcheva, and A. Ruszczyński. *Lectures on Stochastic Programming: Modeling and Theory*. SIAM, 2009.
- [13] B. Defourny, D. Ernst, and L. Wehenkel. *Multistage stochastic programming: A scenario tree based approach to planning under uncertainty*, chapter 6, page 51. Information Science Publishing, Hershey, PA, 2011.
- [14] L.A. Wolsey and G.L. Nemhauser. *Integer and combinatorial optimization*. John Wiley & Sons, 1988.
- [15] SEDG Centre. UK generic distribution system (UKGDS) project. <http://www.sedg.ac.uk/>, 2010.
- [16] R.A. Redner and H.F. Walker. Mixture densities, maximum likelihood and the EM algorithm. *SIAM Review*, 26(2):pp. 195–239, 1984.
- [17] C.M. Bishop. *Pattern recognition and machine learning*. springer, 2006.
- [18] J.-M. Marin, P. Pudlo, C.P. Robert, and R.J. Ryder. Approximate bayesian computational methods. *Statistics and Computing*, 22(6):1167–1180, 2012.
- [19] A. Grelaud, C.P. Robert, J.-M. Marin, F. Rodolphe, and J.-F. Taly. ABC likelihood-free methods for model choice in gibbs random fields. *Bayesian Analysis*, 4(2):317–335, 06 2009.
- [20] E. Jones, T. Oliphant, and P. Peterson. SciPy: Open source scientific tools for Python. 2014.
- [21] F. Pedregosa, G. Varoquaux, A. Gramfort, V. Michel, B. Thirion, O. Grisel, M. Blondel, P. Prettenhofer, R. Weiss, V. Dubourg, and al. Scikit-learn: Machine learning in python. *The Journal of Machine Learning Research*, 12:2825–2830, 2011.
- [22] Trevor Hastie, Robert Tibshirani, Jerome Friedman, and James Franklin. The elements of statistical learning: data mining, inference and prediction. *The Mathematical Intelligencer*, 27(2):83–85, 2005.
- [23] Robert S Garfinkel and George L Nemhauser. *Integer programming*, volume 4. Wiley New York, 1972.
- [24] Yurii Nesterov, Arkadii Nemirovskii, and Yinyu Ye. *Interior-point polynomial algorithms in convex programming*, volume 13. SIAM, 1994.
- [25] W.E. Hart, C. Laird, J.-P. Watson, and D.L. Woodruff. *Pyomo—optimization modeling in python*, volume 67. Springer Science & Business Media, 2012.
- [26] P. Bonami and J. Lee. BONMIN users manual. Technical report, 2006.

- [27] L. Busoniu, D. Ernst, B. De Schutter, and R. Babuska. Cross-entropy optimization of control policies with adaptive basis functions. *IEEE Transactions on Systems, Man, and Cybernetics, Part B: Cybernetics*, 41(1):196–209, 2011.
- [28] D.P. Bertsekas and J.N. Tsitsiklis. *Neuro-Dynamic Programming*. Athena Scientific, Belmont, MA, 1996.
- [29] L. Busoniu, R. Babuska, B. De Schutter, and D. Ernst. *Reinforcement Learning and Dynamic Programming Using Function Approximators*. CRC Press, Boca Raton, FL, 2010.
- [30] W.B. Powell. Clearing the jungle of stochastic optimization. *Informatics Tutorials*, 2014.